Selective Mono-Facial Modification of Graphene Oxide Nanosheets in Suspension

Journal:	*ChemComm*
Manuscript ID	CC-COM-07-2015-005596.R1
Article Type:	Communication
Date Submitted by the Author:	14-Oct-2015
Complete List of Authors:	McGrail, Brendan; Sartomer, R&D Mangadlao, Joey; Case Western Reserve University, Macromolecular Science and Eng. Rodier, Bradley; Case Western Reserve University, Chemistry Swisher, Jordan; Case Western Reserve University, Chemistry Advincula, Gobet; Case Western Reserve University, Macromolecular Science and Eng. Pentzer, Emily; Case Western, Chemistry

Journal Name

COMMUNICATION

Selective Mono-Facial Modification of Graphene Oxide Nanosheets in Suspension

Received 00th January 20xx,
Accepted 00th January 20xx

DOI: 10.1039/x0xx00000x

www.rsc.org/

Brendan T. McGrail,[a] Joey D. Mangadlao,[b] Bradley J. Rodier,[a] Jordan Swisher,[a] Rigoberto Advincula,[b] and Emily Pentzer[a,]*

Graphene oxide (GO) is selectively functionalized on one face to prepare Janus platelets which are characterized by various spectroscopic and microscopic techinques. With this methodology, Janus GO platelets can be prepared without the use of a solid substrate and the two platelet faces can be orthogonally modified in a one-pot reaction.

Structures with two halves or "faces" with distinct properties, such as solubility or chemical reactivity, are commonly called Janus particles. These asymmetric materials are of great interest for applications ranging from complex and tailored self-assembly to directional particle propulsion.[1–3] While Janus structures come in a variety of shapes, spherical structures are most commonly reported, and have been prepared by ligand exchange on inorganic particles, self-assembly of block copolymers, and microfluid methods.[4–7] In contrast to spherical structures, platelets offer higher surface area and the potential for unique and differentiated directional properties based on their aspect ratio.[8] As such, Janus platelets, with the two faces orthogonally functionalized, are an attractive class of materials for their complimentary and contrasting properties compared to spherical Janus particles. To date, the few reported examples of Janus platelets utilize inorganic substrates such as layered silicates.[9–13] Carbon-based Janus platelets (i.e., Janus graphene) have been the subject of theoretical[14,15] studies and have recently been accessed using solid substrates as template.[16–19] As such, a scalable and facile methodology to access Janus platelets is needed.

Graphene oxide (GO), sheets of sp^2 and sp^3 hybridized carbon atoms decorated with oxygen functionalities, offers an exemplary platform for the preparation of Janus platelets. GO is readily accessible in different diameters, can be covalently modified using different chemistries,[21–23] shows good mechanical,[24] medicinal,[25–27] and gas barrier properties,[28] and is a precursor to conductive materials.[29] Moreover, the well-known assembly of GO at the air-water interface in Langmuir-Blodgett (LB) films[30],[31] and oil-water interfaces in Pickering emulsions is well established[32–34] and provides an ideal route to differentiate the two faces of the platelet. To date, such interfacial assembly of GO has been used to prepare hollow GO shells/membranes,[35,36] and armored polymer nanoparticles.[37–41]

Herein, we report the preparation of carbon-based Janus nanosheets using graphene oxide (GO) as a substrate and thiol-ene click chemistry. These Janus platelets are contrasted to non-functionalized and symmetrically functionalized GO using surface-area isotherms and pendant drop tensiometry, and the two faces of the structures are differentiated by X-ray photoelectron spectroscopy (XPS), atomic force microscopy (AFM), and contact angle measurements. We also demonstrate a one-pot method to prepare pH-responsive Janus platelets with the two faces orthogonally functionalized with PS and poly(acrylic acid) (PAA). This work provides a direct, solution-based route to Janus platelets which will be used by researchers across many fields for tailored polymer composites, interfacial stabilization, and dynamic responsive systems.[20]

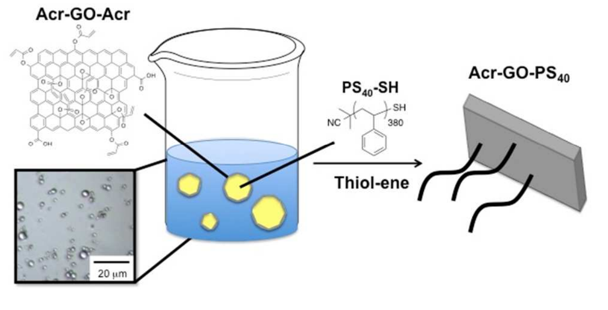

Fig. 1. Preparation of Janus nanosheets of graphene oxide (GO), PS_{40}-GO-Acr, by assembly of Acr-GO-Acr at the toluene-water interface and thiol-ene click using oil-soluble thiol-terminated polystyrene (PS_{40}-SH).

---

[a] *Department of Chemistry, Case Western Reserve University, 10900 Euclid Ave Cleveland, OH 44106. Ebp24@case.edu*

[b] *Department of Macromolecular Science and Engineering, Case Western Reserve University, Cleveland, OH, 44106.*

Electronic Supplementary Information (ESI) available: Characterization data and experimental procedures. See DOI: 10.1039/x0xx00000x

GO was prepared by the modified Hummers method to give platelets ~300-600 nm in diameter with a C:O ratio of ~3:1, as determined by AFM and XPS.[42] Acrylate functionalities were appended to both faces of GO using acrylonitrile in an acidic aqueous environment, as previously reported,[43] to give Acr-GO-Acr. A toluene solution of thiol-terminated polystyrene (PS_{40}-SH, MW =40,000 Da, 10 mg/mL) and Hunig's base was then added to a suspension of these platelets in water and the solution was sonicated to form an emulsion (0.25-1 mg/mL platelets, H_2O:$PhCH_3$ 2:1 vol:vol).[44] Of note, the extent of oxidation (C:O ratio), platelet diameter, solution pH, and ionic strength can all influence the interfacial assembly of GO, and thus the platelet size, extent of oxidation, and oil phase are chosen judiciously.[44,45] In these stabilized emulsions, Acr-GO-Acr platelets lie at the interface between the oil and water phases (Fig. 1) and their relative planarity should prevent flipping when the solution is unagitated, leaving only the acrylate moieties exposed to toluene to react with PS_{40}-SH, and the second, water-exposed face unfunctionalized. Thiol-ene click reaction to give Acr-GO-PS_{40} occurred over the course of ~12 h and successful functionalization confirmed by FTIR and Raman (Fig. S2).[46] For comparison, PS_{40}-GO-PS_{40} was prepared using thiol-ene chemistry in a THF/DMF suspension. The symmetrically functionalized and Janus structures displayed dramatically different solubilities: PS_{40}-GO-PS_{40} readily suspended in THF with mild sonication, while the Janus PS_{40}-GO-Acr only suspended with extended sonication (>1 h) and a solvent mixture of THF/DMF.

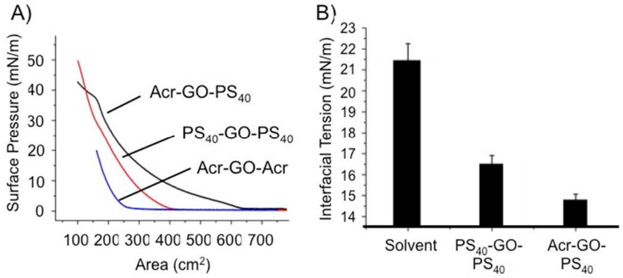

Fig. 2. A) Surface-area isotherms of PS_{40}-GO-Acr Janus GO (black), Acr-GO-Acr (blue), and PS_{40}-GO-PS_{40} (red); B) Interfacial tension pressures of solvent, PS_{40}-GO-PS_{40}, and PS_{40}-GO-Acr from pendant drop tensiometry measurements.

PS_{40}-GO-Acr, Acr-GO-Acr, and PS_{40}-GO-PS_{40} were characterized and contrasted by AFM, π-A isotherms, and pendant drop tensiometry. LB films of each material were collected in the sub-monolayer regime and platelet height was determined by AFM. Dramatically different height profiles were observed for the three samples (Fig. S3): Acr-GO-Acr and PS_{40}-GO-Acr both showed mono-modal distributions of platelet height, with the Janus structures being taller than the unfunctionalized platelets, as expected (4.0 ± 1.4 nm, and 18.2 ± 4.1 nm, respectively). In contrast, PS_{40}-GO-PS_{40} platelets were taller and more disperse (361.8 ± 49.3 nm), suggesting that PS_{40}-GO-PS_{40} platelets aggregate and stack, and do not readily spread into a monolayer on the aqueous subphase.[47] Compression of LB films of the three materials and analysis of the resulting π-A isotherms revealed that Acr-GO-Acr behaves nearly identically to unfunctionalized GO,[31] and PS_{40}-GO-PS_{40} behaves similarly to high molecular weight PS (Fig. 2A, blue and red traces).[47] Both of these symmetric materials are reminiscent of isolated surface particles, with compression leading to a monotonic rise in surface pressure. In contrast, the π-A isotherm of PS_{40}-GO-Acr shows two distinct phase transitions, the first at a high surface area of 630 cm^2 (liquid expanded region) and the second at 158 cm^2 (towards collapse point) (Fig. 2A, black trace), suggesting that the asymmetrically functionalized Janus GO platelets interact with one another in the monolayer at lower concentrations than do Acr-GO-Acr or PS_{40}-GO-PS_{40} platelets.[48] Pendant drop tensiometry measurements (Fig. 2B) further show the difference between the symmetrically functionalized and Janus platelets, with the Janus structures giving rise to lower interfacial tension (i.e., more amphiphilic, though not necessarily a "good" surfactant).

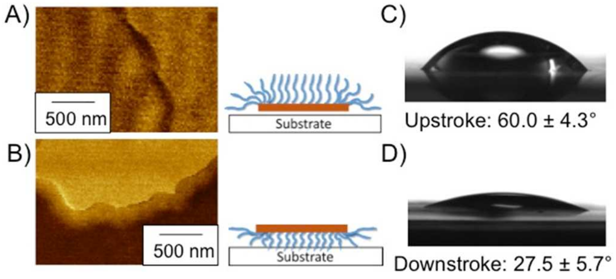

Fig. 3. AFM phase image of PS_{40}-GO-Acr collected by A) upstroke and B) downstroke deposition methods; Water contact angle measurements of PS_{40}-GO-Acr collected by C) upstroke, and D) downstroke deposition methods.

LB monolayers of Janus nanosheets were collected by upstroke and downstroke methods and characterized by XPS, AFM, and contact angle measurements to differentiate the two faces of the platelets. In LB films of the symmetric materials, the same functionality will be exposed to the water and air, while for the Janus structures the acrylate face should be exposed to water and the PS_{40} face exposed to air, based on relative hydrophobicity. Thus, deposition of LB films of PS_{40}-GO-Acr using an upstroke method will present PS_{40} for characterization and downstroke deposition will present the acrylate GO face, giving distinct chemical environments. As expected, the downstroke deposited PS_{40}-GO-Acr has a substantially lower carbon content than that of the upstroke deposited sample (26% vs. 62% respectively, XPS data shown in Fig. S4), and supports the uniqueness of the two faces of Janus platelets. Furthermore, the two faces of PS_{40}-GO-Acr show distinct AFM phase morphology signatures and water contact angles (Fig. 3); in AFM phase images, Janus GO deposited by upstroke methods shows poorly defined platelet edges (Fig. 3A) while the sample deposited by downstroke deposition shows well-defined platelet edges with a poorly defined corona (Fig. 3B), indicating PS_{40} is draped over the platelet edge or the platelet is sitting atop of the polymer, respectively. Further differentiating of the two platelet faces, the contact angle of films deposited by the upstroke method is much larger than those of films deposited by the downstroke method (60.0 ± 4.3° vs. 27.5 ± 5.7°, Fig. 3C and D), as expected since PS is more hydrophobic than acrylated GO. While distinct from each other, the contact angles for both faces of the Janus PS_{40}-GO-Acr fall between extremes defined by spin-coated PS films (~86°)[49] and

Acr-GO-Acr (17.9 ± 2.3°, Fig. S4) which may arise from the "wetting transparency" of graphene,[50] different polymer domains, or the heterogeneity of GO (regions of platelets with a low amount of alcohols and thus low polymer functionalization). Taken together, this data indicates PS_{40}-GO-Acr exposes a hydrophobic, carbon-rich, and polymer-based environment to the air and a GO-like surface the water, supporting the covalent attachment of PS_{40} to only one face and formation of Janus platelets.

Using this new methodology, bi-functional Janus platelets were prepared by performing double thiol-ene reaction on Acr-GO-Acr at the toluene-water interface with water-soluble PAA_5-SH (MW = 5,000 Da) and oil-soluble PS_{40}-SH. The resulting PS_{40}-GO-PAA_5 Janus sheets are expected to stabilize emulsions at high but not low pH, as carboxylic acids are deprotonated and protonated, respectively. As shown in Fig. 4, the difference in emulsion stabilization can be seen by a change in the interfacial tension determined by pendant drop tensiometry (Fig. 4A) and visually (photographs, Fig. 4B and 4C). Under acidic conditions (pH~2), PS_{40}-GO-PAA_5 does not stabilize emulsions due to protonation of carboxylic acid moieties decreasing solubility of the PAA in water. However, under basic conditions (pH~13) and agitation, an emulsion is formed and interfacial tension pressure decreases, assumedly due to carboxylic acid deprotonation to make PAA water soluble. Attempts to use higher molecular weight polymers yielded Janus platelets that were extremely difficult to handle and disperse.

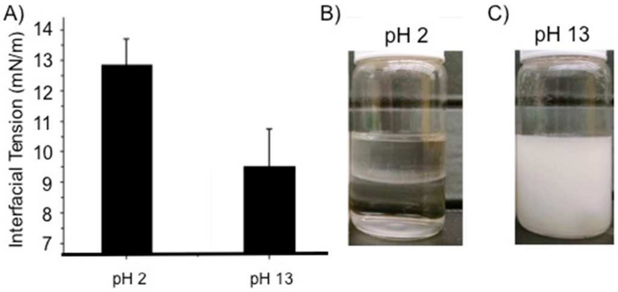

Fig. 4. A) Interfacial tension pressures of PS_{40}-GO-PAA_5 platelets at pH 2 and pH 13; Photographs of PS_{40}-GO-PAA_5 in toluene/water at B) pH 2 and C) pH 13.

In summary, we have prepared Janus GO sheets in solution using thiol-ene click chemistry on functionalized GO assembled at the oil-water interface in Pickering-type emulsions. These PS_{40}-GO-Acr platelets give LB isotherms consistent with surfactants and show lower interfacial tension energy than symmetrically functionalized GO, as determined by pendant drop tensiometry. Furthermore, the two faces of Janus GO (PS_{40} and acrylate) are differentiated by XPS, AFM, and contact angle measurements. Double thiol-ene click on GO platelets at the interface of an emulsion was used to prepare Janus PS_{40}-GO-PAA_5 with distinct interfacial stabilization based on pH. Ongoing work focuses on covalently attaching a variety of polymers and small molecules to either face of the platelets, as well as exploring the influence of size and density of functionality on platelet properties, and determining purity of sample. This novel methodology will be used in a variety of applications, from tailored interfacial properties of GO platelets, to reversible and responsive assemblies, thereby opening avenues for the theoretical, esoteric, and practical investigation of novel platelet systems.

BTM, JS, and EP acknowledge CWRU for financial support. BJR is a NASA Harriett G. Jenkins Pre-doctoral Fellow (Grant #NNX13AR93H). JM and RA acknowledge NSF 0423914 for financial support. AFM and XPS measurements were performed at the Swagelok Center for Surface Analysis of Materials (SCSAM) at CWRU. NMR instrumentation is made possible by NSF MRI-1334048.

Notes and references

[1] A. Walther, A. H. E. Muller, *Chem. Rev.* **2013**, *113*, 5194–5261.
[2] W. Gao, A. Pei, R. Dong, J. Wang, *J. Am. Chem. Soc.* **2014**, *136*, 2276–2279.
[3] X. Yong, E. J. Crabb, N. M. Moellers, A. C. Balazs, *Langmuir* **2013**, *29*, 16066–16074.
[4] C. Lu, M. W. Urban, *ACS Macro Lett.* **2014**, *3*, 346–352.
[5] D. M. Andala, S. H. R. Shin, H.-Y. Lee, K. J. Bishop, *ACS Nano* **2012**, *6*, 1044–1050.
[6] T. S. Skelhon, Y. Chen, S. A. F. Bon, *Langmuir* **2014**.
[7] I. Schick, D. Gehrig, A. Schilmann, H. Bauer, M. Pantho, K. Fischer, D. Strand, F. Laquai, W. Tremel, *J. Am. Chem. Soc.* **2014**, *136*, 2473-2483.
[8] L. Yan, N. Popp, S. Ghosh, A. Bo, *ACSNano* **2010**, *4*, 913–920.
[9] R. Deng, F. Liang, P. Zhou, C. Zhang, X. Qu, Q. Wang, J. Li, J. Zhu, Z. Yang, *Adv. Mater.* **2014**, *26*, 4469–4472.
[10] A. F. Mejia, A. Diaz, S. Pullela, Y.-W. Chang, M. Simonetty, C. Carpenter, J. D. Batteas, M. S. Mannan, A. Clearfield, Z. Cheng, *Soft Matter* **2012**, *8*, 10245–10253.
[11] S. Weiss, D. Hirsemann, B. Biersack, M. Ziadeh, A. H. E. Müller, J. Breu, *Polymer.* **2013**, *54*, 1388–1396.
[12] D. Hirsemann, S. Shylesh, R. a De Souza, B. Diar-Bakerly, B. Biersack, D. N. Mueller, M. Martin, R. Schobert, J. Breu, *Angew. Chem. Int. Ed. Engl.* **2012**, *51*, 1348–1352.
[13] Y. Liu, F. Liang, Q. Wang, X. Qu, Z. Yang, *Chem. Commun.* **2015**, *51*, 3562–3565.
[14] M. Yang, R. Zhao, J. Wang, L. Zhang, Q. Xie, Z. Liu, Z. Liu, *J. Appl. Phys.* **2013**, *113*, 084313.
[15] J. Zhou, M. M. Wu, X. Zhou, Q. Sun, *Appl. Phys. Lett.* **2009**, *95*, 103108.
[16] L. Zhang, J. Yu, M. Yang, Q. Xie, H. Peng, Z. Liu, *Nat. Commun.* **2013**, *4*, 1443.
[17] D. Yu, E. Nagelli, R. Naik, L. Dai, *Angew. Chem. Int. Ed. Engl.* **2011**, *50*, 6575–6578.
[18] H. Wu, W. Yi, Z. Chen, H. Wang, Q. Du, *Carbon* **2015**, *93*, 473–483.
[19] D. Han, P. Xiao, J. Gu, J. Chen, Z. Cai, J. Zhang, W. Wang, T. Chen, *RSC Adv.* **2014**, 22759–22762.
[20] M. Cui, T. Emrick, T. P. Russell, *Science.* **2013**, *342*, 460–463.
[21] L. Liao, H. Peng, Z. Liu, *J. Am. Chem. Soc.* **2014**, *136*, 12194–12200.
[22] H. J. Salavagione, G. Martínez, G. Ellis, *Macromol. Rapid Commun.* **2011**, *32*, 1771–1789.
[23] V. Georgakilas, M. Otyepka, A. B. Bourlinos, V. Chandra, N. Kim, K. C. Kemp, P. Hobza, R. Zboril, K. S. Kim, *Chem. Rev.* **2012**, *112*, 6156–6214.
[24] X. Sun, H. Sun, H. Li, H. Peng, *Adv. Mater.* **2013**, *25*, 5153–76.
[25] H. Y. Mao, S. Laurent, W. Chen, O. Akhavan, M. Imani, A. A. Ashkarran, M. Mahmoudi, *Chem. Rev.* **2013**, *113*, 3407–3424.
[26] I. E. Mejias Carpio, J. D. Mangadlao, H. N. Nguyen, R. C. Advincula, D. F. Rodrigues, *Carbon* **2014**, *77*, 289–301.
[27] J. D. Mangadlao, C. M. Santos, M. J. L. Felipe, a C. C. de Leon, D. F. Rodrigues, R. C. Advincula, *Chem. Commun.* **2015**, *51*, 2886–2889.
[28] Y.-H. Yang, L. Bolling, M. a Priolo, J. C. Grunlan, *Adv. Mater.* **2013**, *25*, 503–508.
[29] C. K. Chua, M. Pumera, *J. Mater. Chem. A* **2013**, *1*, 1892–1898.
[30] C. Chen, Q.-H. Yang, Y. Yang, W. Lv, Y. Wen, P.-X. Hou, M. Wang, H.-M. Cheng, *Adv. Mater.* **2009**, *21*, 3007–3011.
[31] L. J. Cote, F. Kim, J. Huang, *J. Am. Chem. Soc.* **2009**, *131*, 1043–1049.
[32] J.-J. Shao, W. Lv, Q.-H. Yang, *Adv. Mater.* **2014**, *26*, 5586–612.
[33] J. Kim, L. J. Cote, F. Kim, W. Yuan, K. R. Shull, J. Huang, *J. Am. Chem. Soc.* **2010**, *132*, 8180–8186.
[34] F. Kim, L. J. Cote, J. Huang, *Adv. Mater.* **2010**, *22*, 1954–1958.
[35] P. Guo, H. Song, X. Chen, *J. Mater. Chem.* **2010**, *20*, 4867–4874.
[36] Y. Zhang, X. Zheng, H. Wang, Q. Du, *J. Mater. Chem. A* **2014**, *2*, 5304–5314.
[37] X. Song, Y. Yang, J. Liu, H. Zhao, *Langmuir* **2011**, *27*, 1186–1191.

[38] M. M. Gudarzi, F. Sharif, *Soft Matter* **2011**, *7*, 3432–3440.
[39] L. Zhang, T. Shi, S. Wu, H. Zhou, *High Perform. Polym.* **2015**, *26*, 156–165.
[40] H. M. Etmimi, R. D. Sanderson, *Macromolecules* **2011**, *44*, 8504–8515.
[41] H. Hu, X. Wang, J. Wang, L. Wan, F. Liu, H. Zheng, R. Chen, C. Xu, *Chem. Phys. Lett.* **2010**, *484*, 247–253.
[42] D. C. Marcano, D. V Kosynkin, J. M. Berlin, A. Sinitskii, Z. Sun, A. Slesarev, L. B. Alemany, W. Lu, J. M. Tour, *ACS Nano* **2010**, *4*, 4806–4814.
[43] B. T. McGrail, B. J. Rodier, E. Pentzer, *Chem. Mater.* **2014**, *26*, 5806–5811.
[44] Y. He, F. Wu, X. Sun, R. Li, Y. Guo, C. Li, L. Zhang, F. Xing, W. Wang, J. Gao, *ACS Appl. Mater. Interfaces* **2013**, *5*, 4843–4855.
[45] D. R. Dreyer, A. D. Todd, C. W. Bielawski, *Chem. Soc. Rev.* **2014**, *43*, 5288–5301.
[46] L. M. Campos, K. L. Killops, R. Sakai, J. M. J. Paulusse, D. Damiron, E. Drockenmuller, B. W. Messmore, C. J. Hawker, *Macromolecules* **2008**, *41*, 7063–7070.
[47] J. Kumaki, *Macromolecules* **1988**, *21*, 749–755.
[48] J. Y. Park, R. C. Advincula, *Soft Matter* **2011**, *7*, 9829.
[49] Y. Li, J. Q. Pham, K. P. Johnston, P. F. Green, *Macromolecules* **2007**, *22*, 9785–9793.
[50] J. Rafiee, X. Mi, H. Gullapalli, A. V Thomas, F. Yavari, Y. Shi, P. M. Ajayan, N. A. Koratkar, *Nat. Mater.* **2012**, *11*, 217–222.